

Nanoscale

Accepted Manuscript



This is an *Accepted Manuscript*, which has been through the Royal Society of Chemistry peer review process and has been accepted for publication.

Accepted Manuscripts are published online shortly after acceptance, before technical editing, formatting and proof reading. Using this free service, authors can make their results available to the community, in citable form, before we publish the edited article. We will replace this *Accepted Manuscript* with the edited and formatted *Advance Article* as soon as it is available.

You can find more information about *Accepted Manuscripts* in the [Information for Authors](#).

Please note that technical editing may introduce minor changes to the text and/or graphics, which may alter content. The journal's standard [Terms & Conditions](#) and the [Ethical guidelines](#) still apply. In no event shall the Royal Society of Chemistry be held responsible for any errors or omissions in this *Accepted Manuscript* or any consequences arising from the use of any information it contains.

1 **Carbon coating may expedite the fracture of carbon-coated** 2 **silicon core-shell nanoparticles during lithiation**†

3 Weiqun Li,^a Ke Cao,^b Hongtao Wang,^c Jiabin Liu,^b Limin Zhou,^a Haimin Yao^{*,a}

4
5 Previous studies on silicon (Si) indicate the lithiation-induced fracture of crystalline Si
6 nanoparticles can be greatly inhibited if their diameter is reduced to below a critical
7 length scale around 150 nm. In this paper, *in situ* lithiation of individual carbon-coated Si
8 nanoparticles (Si@C NPs) is conducted and shows that Si@C NPs will fracture during
9 lithiation even though the diameter is much smaller than 150 nm, implying a deleterious
10 effect of the carbon coating on the integrity of the Si@C NPs during lithiation. To shed
11 light on this effect, finite element analysis is carried out and reveals that the carbon
12 coating, if fractured during lithiation, will induce cracks terminating at the C/Si interface.
13 Such cracks, upon further lithiation, can immediately propagate into the Si core due to the
14 elevated driving force caused by material inhomogeneity between the coating and core.
15 To prevent the fracture of the carbon coating so as to protect the Si core, a design
16 guideline is proposed by controlling the ratio between the diameter of Si core and the
17 thickness of carbon coating. The results in this paper should be of practical value to the

^a *Department of Mechanical Engineering, The Hong Kong Polytechnic University, Hung Hom, Kowloon, Hong Kong SAR, P.R. China. E-mail: mmhyao@polyu.edu.hk; Fax: +852-2365 4703; Tel: +852-2766 7817*

^b *School of Materials Science and Engineering, Zhejiang University, Hangzhou 310027, P.R. China*

^c *Institute of Applied Mechanics, Zhejiang University, Hangzhou 310027, P.R. China*

† Electronic Supplementary Information (ESI) available: details of finite element simulations including analogous treatment of lithiation-induced expansion, calculation of energy release rate and effect of material's inhomogeneity on it.

18 design and application of Si-based core-shell structured anode materials for lithium ion
19 batteries.

20 **1. Introduction**

21 Recently, techniques for storage of electrical energy have been developing rapidly,
22 leading to a wide application in many fields such as portable electronic devices, electric
23 vehicles and so on. Lithium ion battery (LIB), due to its high energy density, is
24 recognized as the one of the most promising devices for electrical energy storage.¹
25 Among diverse electrode materials for LIB, silicon (Si) stands out for its high capacity (~
26 4200 mAh g⁻¹), abundant reserves (~28% of the total mass of the earth's crust) and low
27 cost.² However, the wide application of Si as the electrode material of LIB is still
28 impeded by its Achilles' heel: the large volume expansion (~400%) during lithiation and
29 delithiation which will cause the fracture and pulverization of the electrode materials and
30 delamination of the interface between the electrode material and periphery structures
31 such as current collector, resulting in poor conductivity and rate capability, short cycle
32 life and even overall failure of the battery.^{3,4} Although nanoscale Si particles have been
33 shown to have the capability to resist fracture during lithiation,^{5,6} the large volume
34 change of Si electrode would cause repeated fracture and formation of the solid-
35 electrolyte interphase (SEI) layer on the Si electrode surface during lithiation and
36 delithiation. This process not only leads to the thickening of the SEI layer therefore
37 lowers the electronic and ionic conductivity and coulombic efficiency, but also consumes
38 the Si and electrolyte and finally results in the dry-out of the cell.⁷ To solve these
39 problems, coating such as carbon has been imposed on the Si to constrain its volume
40 expansion and also prevent the direct contact between the Si and the electrolyte.⁸⁻¹⁴ As a

41 consequence, the electronic and ionic conductivity is improved and a much more stable
42 SEI film forms on the carbon coating surface as long as the structural integrity of coating
43 is maintained. Otherwise, if the carbon coating is cracked during electrochemical cycling,
44 the coating will lose its efficacy as new SEI layer will form and thicken on the electrode
45 surfaces. Therefore, maintaining the structural integrity of carbon coating on the Si
46 electrode materials is significantly important for the application of the carbon-coated Si
47 nanoparticles (Si@C NPs) as the electrode materials for LIB.

48 In this paper, Si@C NPs were synthesized, on which *in situ* lithiation tests were
49 conducted using transmission electron microscopy (TEM).^{15,16} The Si@C NPs were
50 found to fracture even though the diameter of the crystalline Si core is much lower than
51 150 nm, which has been deemed as the maximum size of bare crystalline Si NPs capable
52 of maintaining integrity during lithiation.⁵ Finite element simulation¹⁷⁻¹⁹ was used to
53 account for such deleterious effect of carbon coating on the structural integrity of Si@C
54 NPs, giving rise to a guideline for designing Si@C NPs with high persistence to
55 structural integrity during lithiation.

56 **2. Experimental**

57 *2.1. Synthesis of carbon-coated silicon nanoparticles*

58 Si@C NPs were synthesized by using sucrose as the carbon source.²⁰ 100 mg Si
59 NPs and 600 mg sucrose were firstly dissolved in a solution made of 0.6 mL hydrochloric
60 acid (37 wt%), 6 mL deionized water and 8 mL absolute ethanol (99.9 wt%) under
61 stirring and then ultrasonicated for 120 mins. Subsequently, the solution was stirred at
62 70 °C for 3 hours and then dried in vacuum oven at 120 °C for 8 hours. The as-prepared
63 Si-sucrose product was loaded in an alumina crucible after manual grinding. Then, the

64 crucible was moved into the furnace and heated at 800 °C for 2 hours and cooled down to
65 room temperature under the protection of nitrogen atmosphere.

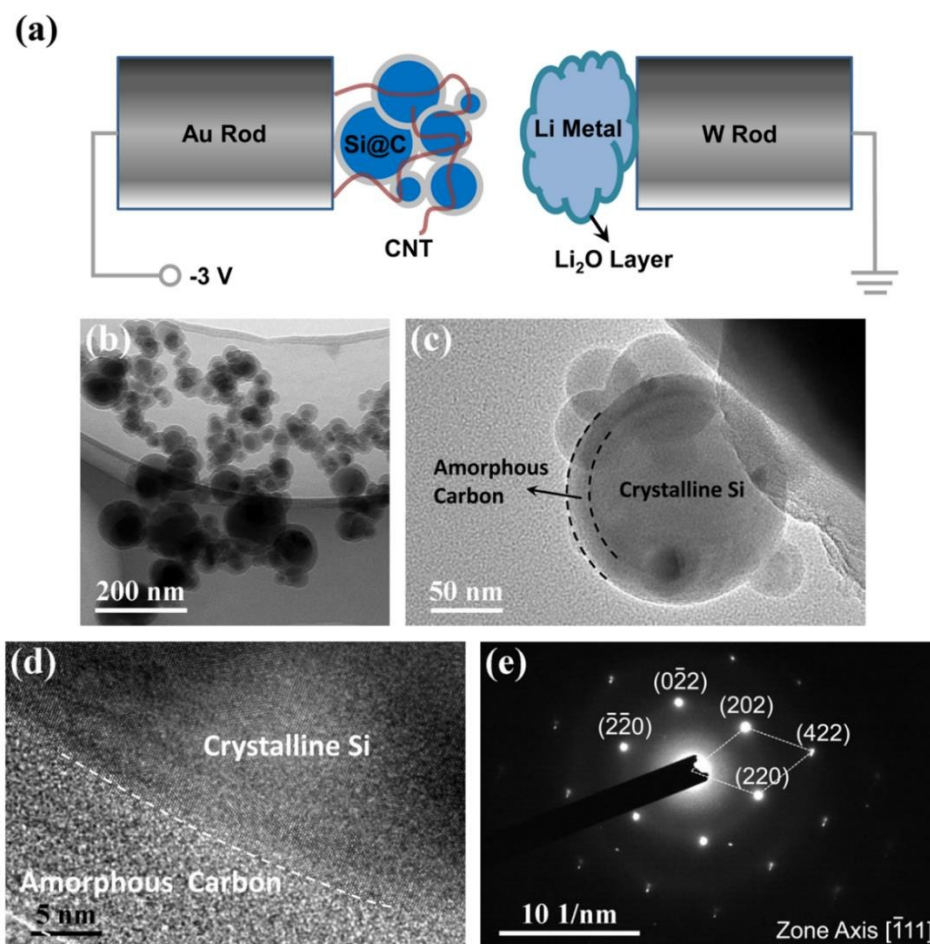
66 2.2. *In situ* TEM observation

67 The *in situ* lithiation test was conducted on the Si@C NPs in a TEM (JEM-2100,
68 JEOL) equipped with a Nanofactory® STM-TEM holder. Fig. 1a shows the schematic of
69 the nanoscale battery setup of the solid electrochemical cell for lithiation,^{4,6} in which the
70 Si@C NPs are attached onto the flat-ended gold rod (~200 μm in diameter) with silver
71 paste. To improve the electronic conductivity, a small amount of carbon nanotubes (CNT)
72 were added into the Si@C NPs. The counter electrode was a piezo-driven tungsten probe
73 covered with Li metals. The surface layer of the Li metal was unavoidably oxidized to
74 Li₂O during the handling in air and the resulting Li₂O layer served as solid electrolyte.
75 The intensity of electron beam was minimized to avoid the decomposition of Li₂O layer,
76 prevent the direct contact between the Li metal and the Si@C NPs and therefore
77 guarantee the electrochemical reaction rather than the chemical reaction between Li and
78 Si@C NPs.⁵ With the aid of TEM, a nano contact was made between the Li metal and the
79 Si@C NPs and a larger external bias (−3 V), in comparison with that in the actual LIB,
80 was then applied to initiate the lithiation, leading to the Li⁺ transportation through the
81 Li₂O layer, the insertion of Li⁺ into the carbon coating and then into the Si core, and the
82 phase transition from Si to lithiated Si.²¹ The electrochemical reaction and the diffusion
83 of Li⁺ here are similar to those in the actual LIB.^{4,6} Therefore, the nano battery can
84 effectively simulate the real reaction and structural change in the actual LIB.

85 3. Results and discussion

86 3.1. Experimental observation

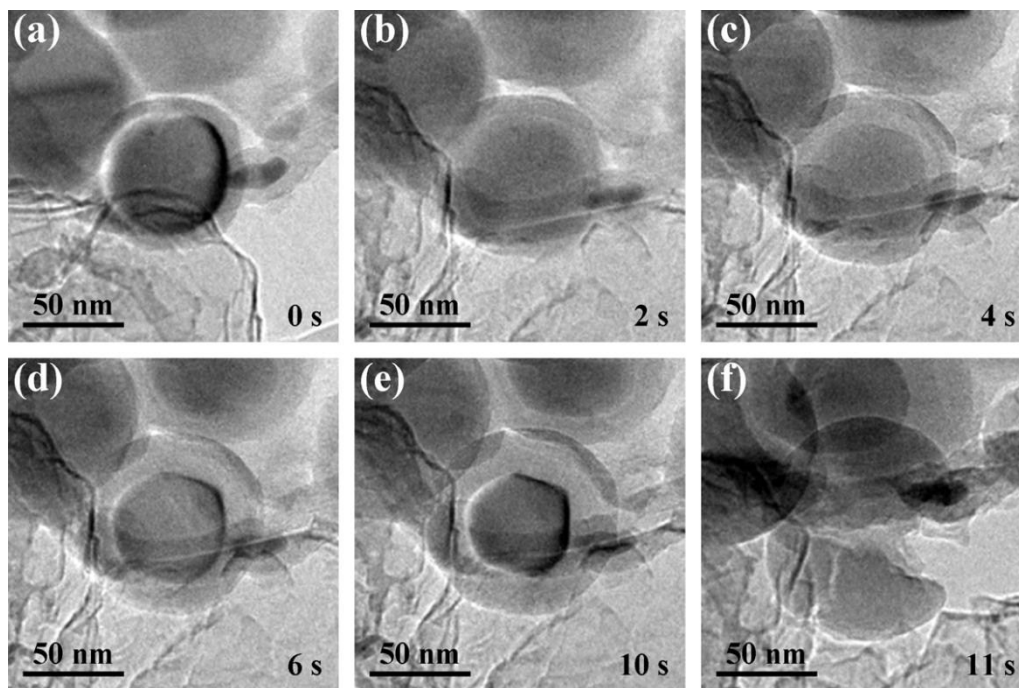
87 Figs. 1b and c show the TEM images of the synthesized Si@C NPs under different
 88 magnifications. It can be seen that the Si@C NPs exhibit inhomogeneity in both the
 89 diameter of the Si core and the thickness of the carbon coating. *In situ* measurements
 90 indicate that the diameter of the Si core ranges from 10 to 150 nm while the carbon
 91 coating is about 5 to 15 nm in thickness. Moreover, the high resolution TEM image of a
 92 typical Si@C NP in Fig. 1d indicates that the carbon coating is amorphous, while the Si
 93 core is crystalline with high crystallinity confirmed by the selected area electron
 94 diffraction (SAED) pattern (Fig. 1e).



95

96 **Fig. 1 (a) Schematic of the setup of *in situ* lithiation test; (b, c) TEM images of the**
97 **Si@C NPs under different magnifications; (d) high resolution TEM image showing**
98 **the amorphous carbon coating and the crystalline Si core as confirmed by the SAED**
99 **pattern in (e).**

100 Figs. 2a-f show the snapshots of the lithiation process of a Si@C NP with diameter
101 of Si core about 60 nm and thickness of carbon coating around 9 nm. It was reported that
102 bare crystalline Si NP with diameter smaller than 150 nm will not fracture during
103 lithiation.⁵ Unexpectedly, our *in situ* lithiation test showed that Si@C NP tends to
104 fracture during lithiation even though the diameter of the Si core is only 60 nm. That is,
105 carbon coating induces, rather than inhibits, the fracture of Si core and therefore plays a
106 deleterious role in maintaining the integrity of Si@C NP during lithiation.

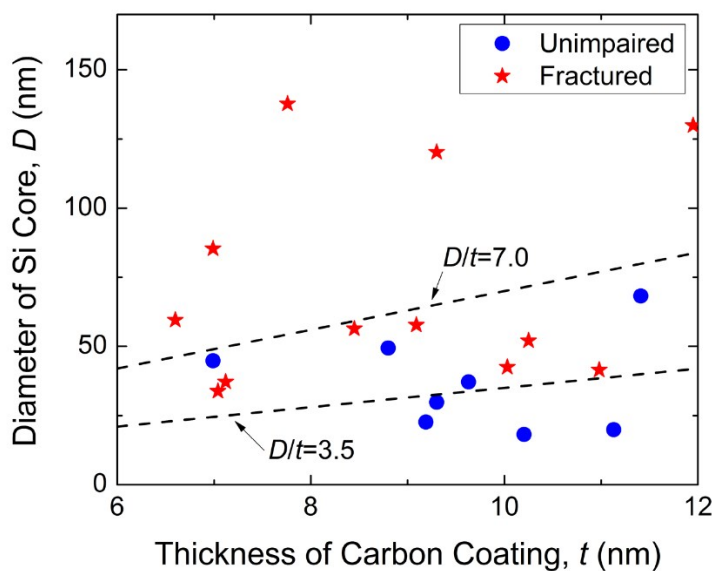


107

108 **Fig. 2 Temporal evolution of the morphology of Si@C NP during *in situ* lithiation.**

109 We repeated the *in situ* lithiation test on many Si@C NPs and found that lithiation
110 may not necessarily lead to the fracture of Si@C NPs. Fig. 3 summarizes the events with

111 and without fracture on a D - t plane for all the tested Si@C NPs, where D refers to the
 112 diameter of the Si core and t stands for the thickness of the carbon coating. It can be seen
 113 that whether the Si@C NPs fracture or not after lithiation depends not only on the
 114 diameter of the Si core but also on the thickness of the carbon coating. A general trend
 115 implied by Fig. 3 is that Si@C NPs with larger D and smaller t tend to fracture during
 116 lithiation. Further examination on Fig. 3 indicates that the ratio between D and t may play
 117 an essential role in dominating the occurrence of fracture because fracture happens in all
 118 Si@C NPs with $D/t > 7.0$ while no fracture is observed in any Si@C NP with $D/t < 3.5$.
 119 For the Si@C NPs with intermediate D/t ranging from 3.5 to 7.0, the occurrence of
 120 fracture seems random. It can be inferred that there exists a critical ratio of D/t , below
 121 which fracture of Si@C NP can be prohibited. A rough estimation of such critical ratio of
 122 D/t obtained from Fig. 3 is a number between 3.5 and 7.0.



123

124 **Fig. 3 Dependence of fracture of Si@C NP on the diameter of Si core and thickness**
 125 **of carbon coating.**

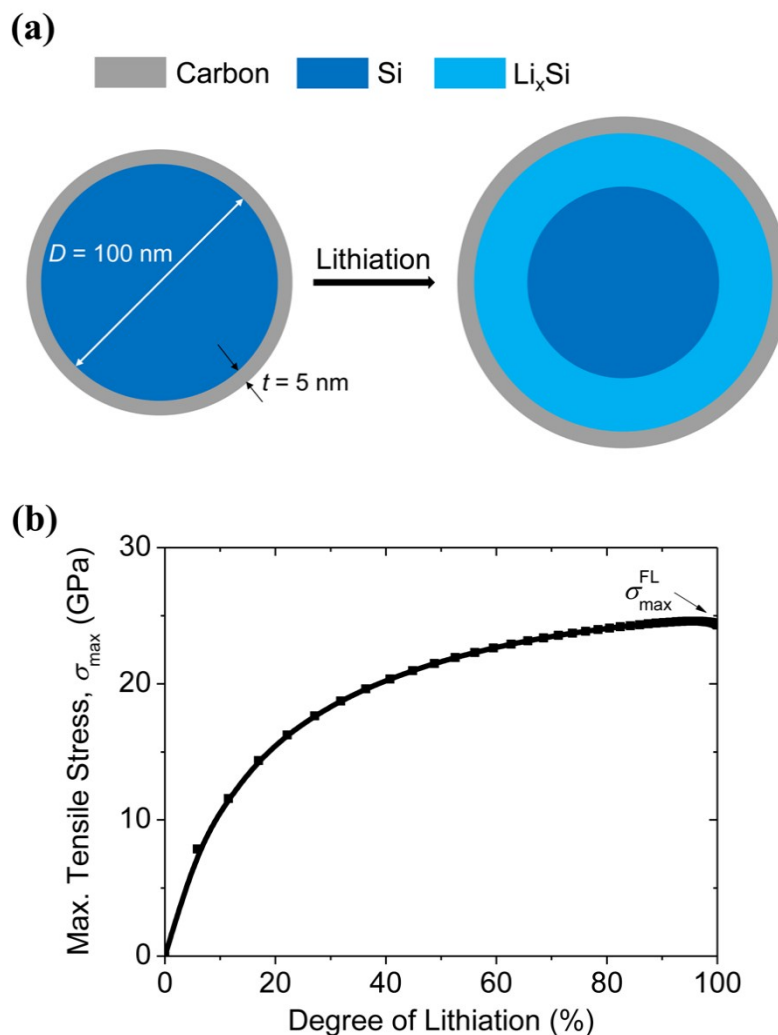
126

127 3.2. Finite element analysis

128 In order to shed light on the fracture mechanism of Si@C NPs during lithiation
129 especially for those with diameters much smaller than 150 nm, finite element analysis
130 (FEA) was carried out. Fig. 4a shows the FEA model we applied, in which a Si@C NP
131 (2-D) consists of a Si core with diameter of 100 nm and carbon coating with thickness of
132 5 nm. We firstly examined the stress developed in the carbon coating during lithiation.
133 By following the approach of analogy we developed in our earlier work,¹⁹ the lithiation-
134 induced volume expansion can be equivalently treated as thermal expansion caused by a
135 prescribed increment of the temperature field simulating the increase of Li⁺ concentration.
136 We neglected the lithiation of the carbon coating and assumed that the lithiation of Si
137 core starts from its external periphery and advances symmetrically towards its center. The
138 frontier of the lithiated region was assumed sharp.²²⁻²⁵ That is, the core was either pristine
139 (unlithiated) Si or fully lithiated Si (Li_xSi). We assumed that the carbon coating was pure
140 elastic while the Si and Li_xSi were elastic-perfectly-plastic with mechanical properties
141 taken as the values shown in Table 1. The Si and carbon coating were assumed perfectly
142 bonded and no delamination was allowed on their interface. This assumption was based
143 on our observation that no delamination happened between lithiated Si and carbon during
144 *in situ* lithiation experiments. Such strong interfacial bonding between lithiated Si and
145 carbon has also been reported in literature¹¹ and may be due to the interpenetration of Si
146 and carbon near their interface as shown in Fig. 1d.

147 **Table 1. Typical mechanical properties taken in FEA simulations**

| Materials | Young's modulus (GPa) | Poisson's ratio | Yield strength (GPa) |
|--------------------|-----------------------|--------------------|----------------------|
| Carbon | 300 ²⁶ | 0.25 ²⁶ | - |
| Si | 169 ²⁷ | 0.26 ²⁷ | 7 ²⁸ |
| Li _x Si | 3.5 ²⁹ | 0.23 ³⁰ | 0.5 ^{31,32} |

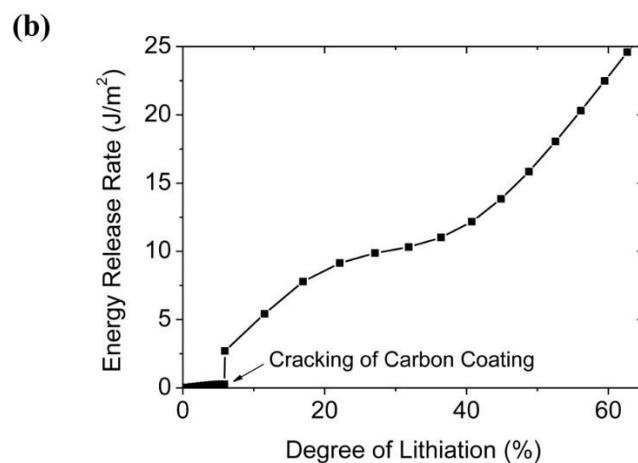
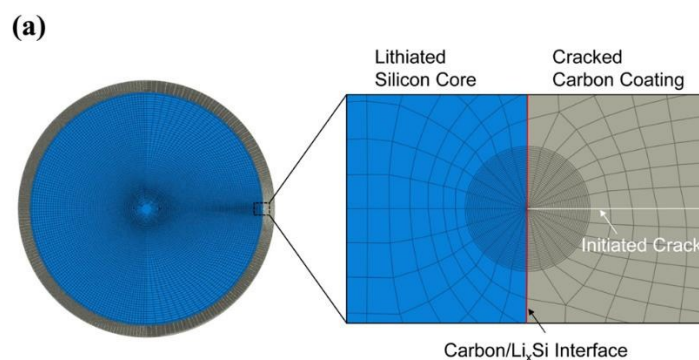


148

149 **Fig. 4 (a) Schematic of FEA model of Si@C NP for evaluating the stress developed**
 150 **in the carbon coating during lithiation; (b) Variation of the maximum tensile stress**
 151 **(σ_{\max}) in the carbon coating of Si@C NP with lithiation. $\sigma_{\max}^{\text{FL}}$ here denotes the**
 152 **maximum tensile stress in the carbon coating at the full lithiation moment.**

153 To simulate the process of lithiation, the Si core was discretized into many
 154 concentric thin annuluses. Prescribed incremental “temperature” was applied on these
 155 thin annuluses one after another in the order from outside to inside, modelling the inward
 156 diffusion of the Li^+ . The calculated results were found dependent on the number of the
 157 discrete annuluses or the annulus thickness, but convergent results can be obtained if the

158 thickness of the discrete annuluses is made sufficiently thin (Fig. S1†). Fig. 4b shows the
159 evolution of the calculated maximum tensile stress, σ_{\max} , in the carbon coating, which is
160 along the hoop direction and is located near the carbon/ Li_xSi interface, with the degree of
161 lithiation. Here, degree of lithiation is defined as the fraction of the Si that has been
162 lithiated. That is, 100% lithiation means fully lithiated. Fig. 4b indicates that the σ_{\max} in
163 the carbon coating increases with the degree of lithiation and almost saturates at ~25 GPa
164 after 80% lithiation. According to the maximum-tensile-stress criterion of fracture for
165 brittle materials,³³ the carbon coating will fracture if the σ_{\max} reaches its fracture strength
166 σ_f . For amorphous carbon, it was reported that σ_f ranges from 7 to 30 GPa.^{26,34} If we
167 take 7 GPa as a conservative estimation, Fig. 4b implies that fracture may take place
168 around 6% lithiation.



169

170 **Fig. 5 (a) Meshed finite element model for calculating the energy release rate (J -**
171 **integral) near the tip of a crack terminating at the carbon/lithiated Si interface; (b)**
172 **Calculated energy release rate (J -integral) as a function of the degree of lithiation.**

173 Once the carbon coating is fractured, a crack terminating at the carbon/Li_xSi
174 interface forms. As the bonding between the lithiated Si and carbon is normally strong,¹¹
175 the formed crack is prone to penetrating into the lithiated Si rather than deflecting along
176 the carbon/lithiated Si interface. To estimate the subsequent evolution of the crack,
177 driving force for crack propagation was examined by calculating the J -integral³⁵ around
178 the crack tip, as shown in Fig. 5a. The calculated evolution of the J -integral with the
179 lithiation is shown in Fig. 5b. Based on the preceding analysis of the σ_{\max} developed in
180 the carbon coating, the cracking of carbon coating happens at the moment of 6%
181 lithiation. Therefore, substantial J -integral is only observed after 6% lithiation. It can be
182 seen that the J -integral increases rapidly with lithiation. It reaches up to more than 10 J
183 m⁻² at ~30% lithiation. That is, the J -integral can reach a considerable level upon a small
184 amount of further lithiation after the cracking of the carbon coating. Recalling that the
185 critical energy release rate for crack growth, or the fracture toughness, for lithiated Si is
186 about 10 J m⁻²,^{36,37} the J -integral near the crack tip can easily exceed this value, leading to
187 the penetration of crack into the core and therefore the fracture of the whole Si@C NP.
188 Such high energy release rate is mainly due to the material's inhomogeneity along the
189 direction of crack extension, namely the dissimilarity between the carbon coating and
190 lithiated Si in mechanical properties.³⁸ Earlier analysis in fracture mechanics indicated
191 that material inhomogeneity could lead to either a shielding or anti-shielding effect on the
192 crack propagation, depending on the directionality of inhomogeneity. If the crack tends to
193 propagate from stiff/hard material to compliant/soft material, the material inhomogeneity

194 would facilitate the crack propagation. On the contrary, if the crack tends to propagate
195 from compliant/soft material to stiff/hard material, the material inhomogeneity would
196 prohibit the crack propagation.³⁸ Clearly, our case belongs to the former scenario because
197 the carbon coating is stiffer and harder compared to the lithiated Si. A comparison was
198 made between the energy release rates developed in a cracked Si@C NP and a cracked
199 uncoated Si NP during lithiation. The results (Fig. S2†) show that the energy release rate
200 in the uncoated Si NP, which has no material inhomogeneity, is much lower than that in a
201 Si@C NP shown above even though the NPs and the preexisting cracks have the same
202 size. Therefore, the carbon coating on the Si@C NP, if fractured, will expedite the
203 fracture of the whole Si@C NP.

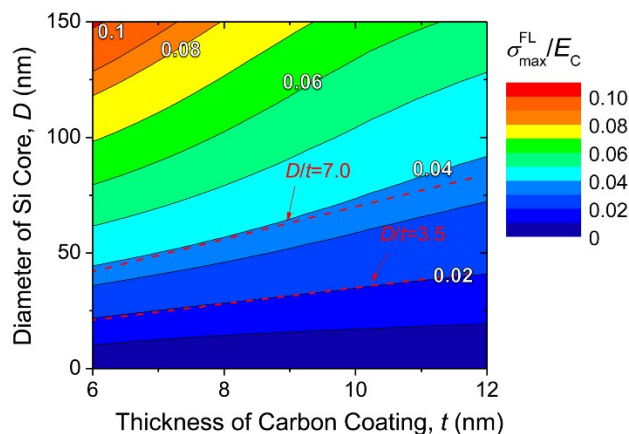
204 It should be pointed out that in our simulation the calculated J -integrals were found
205 to have certain path-dependence. At given lithiation level, the calculated J -integral
206 decreases with the distance of the path from the crack tip (Fig. S3†). When the path is
207 sufficient far away from the crack tip, convergent J -integral is obtained, which is taken as
208 the energy release rate shown in Fig. 5b.

209

210 3.3. Optimal design of Si@C NP

211 Above analysis indicates that the crack in the carbon coating, once developed, is
212 quite easy to propagate into the Si core. To prevent the Si@C NP from fracturing, the
213 integrity of the carbon coating should be secured, which can be achieved by optimizing
214 the geometries of the Si@C NP. By adopting different diameters of the Si core (D) and
215 thicknesses of the carbon coating (t) in the FEA model shown in Fig. 4a, we conducted a
216 parametric study on the effects of D and t on the $\sigma_{\max}^{\text{FL}}$ developed in the carbon coating

217 during lithiation. Here $\sigma_{\max}^{\text{FL}}$ refers to the maximum tensile stress in the carbon coating at
218 the full lithiation moment, as illustrated in Fig. 4b. Fig. 6 shows the normalized $\sigma_{\max}^{\text{FL}}$ as a
219 function of D and t . It can be seen that larger D and smaller t result in higher $\sigma_{\max}^{\text{FL}}$. This
220 trend agrees well with the observation from the *in situ* lithiation that Si@C NPs with
221 larger core diameter and thinner coating thickness tend to fracture more easily during
222 lithiation (Fig. 3). To prevent the fracture of the carbon coating, one should control the
223 $\sigma_{\max}^{\text{FL}}$ below the fracture strength of carbon σ_f . For given σ_f , Fig. 6 implies an
224 “unimpaired region” on the D - t plane in which the $\sigma_{\max}^{\text{FL}}$ is lower than σ_f or the integrity
225 of carbon coating can be ensured. For example, if we take $\sigma_f = 6$ GPa and
226 $E_C = 300$ GPa, the region below the contour line of $\sigma_{\max}^{\text{FL}} / E_C = 0.02$ in Fig. 6 is the
227 “unimpaired region”. Interestingly, it can be seen that the contour line of 0.02 in Fig. 6
228 almost coincides with the line defined by $D/t = 3.5$. Similarly, the contour line
229 corresponding to $\sigma_{\max}^{\text{FL}} / E_C = 0.04$ is quite close to the line defined by $D/t = 7.0$.
230 Comparing Fig. 6 and Fig. 3, it can be predicted that the fracture strength of the carbon
231 coating in our Si@C NPs ranges from 6 to 12 GPa, which agrees well with the value
232 reported in the literature.³⁴ This prediction also justifies our earlier selection of
233 $\sigma_f = 7$ GPa when predicting the critical degree of lithiation causing fracture of carbon
234 coating for the model in Fig. 4a.



235

236 **Fig. 6 Maximum tensile stress at full lithiation in the carbon coating of Si@C NPs**
 237 **with different core diameters D and coating thicknesses t . Here, $\sigma_{\max}^{\text{FL}}$ is normalized**
 238 **by $E_C = 300$ GPa.**

239

240 Although Fig. 6 indicates that lower value of D/t is preferential for prohibiting the
 241 fracture of Si@C NPs, the demand for high capacity on the contrary requires higher D/t
 242 because Si possesses much higher theoretical capacity compared to carbon. The optimal
 243 value of D/t catering for both requirements above is the maximum mechanically
 244 allowable D/t . For our case, a conservative estimation of the optimal D/t from Fig. 6 is
 245 3.5.

246 4. Conclusions

247 In this paper, *in situ* lithiation was carried out on the synthesized Si@C NPs. It was
 248 observed that lithiation could cause fracture of Si@C NPs with diameters smaller than
 249 150 nm, which has been viewed as the maximum allowable size of bare Si nanoparticles
 250 immune to lithiation-induced fracture. Such deleterious effect of carbon coating on the
 251 integrity of Si@C NP was analyzed using FE simulation. Our results indicated that the

252 maximum tensile stress experienced by the carbon coating of Si@C NP during the
253 lithiation process depends on the size of the Si core as well as the thickness of the carbon
254 coating. Excessive tensile stress will be readily developed in the carbon coating if the Si
255 core is too large or the carbon coating is too thin, leading to the fracture of the carbon
256 coating. The resulting crack in the carbon coating will experience an elevated driving
257 force for growth due to the unfavorable material inhomogeneity between the carbon
258 coating and the lithiated Si, inducing the fracture of the whole Si@C NP. To secure the
259 structural integrity of Si@C NP during lithiation and meanwhile attain capacity as high as
260 possible, a design guideline for Si@C NP is proposed by controlling the ratio between the
261 Si core diameter and the carbon coating thickness below a critical value. Our discussion
262 above was based on the assumption that the carbon coating and lithiated Si were perfectly
263 bonded. Recently, people developed slidable layered graphene coating on Si¹² and yolk-
264 shell architecture,¹⁰ in which the carbon/Si interface was weak or even vanishing. These
265 innovations provide alternative solutions for solving the fracture problem of electrode
266 materials during lithiation. Admittedly, our results provided a necessary but not a
267 sufficient condition for the long cycle life of the Si@C NP electrode materials since we
268 only considered the integrity of the carbon coating during the first lithiation. The fatigue
269 stability of electrode materials upon cyclic lithiation and delithiation loading, the
270 interactions between the electrode materials and the current collector and the formation
271 and stability of SEI layers have not been considered fully and require further studies.

272

273 **Acknowledgements**

274 This work was supported by the General Research Fund from Hong Kong RGC
275 (529313). HW would like to acknowledge the support from the National Natural Science
276 Foundation of China (11322219, 11321202). WL acknowledges Mr. Zheng-Long Xu and
277 Prof. Jang-Kyo Kim from the Hong Kong University of Science and Technology for the
278 helpful discussion on the lithiation-induced fracture of Si@C nanoparticles, and Dr. Wei
279 Lu from the Materials Research Center of the Hong Kong Polytechnic University for
280 providing technical supports.

281 **References**

- 282 1 A. S. Aricò, P. Bruce, B. Scrosati, J.-M. Tarascon and W. van Schalkwijk, *Nat.*
283 *Mater.*, 2005, **4**, 366-377.
- 284 2 M. T. McDowell, S. W. Lee, W. D. Nix and Y. Cui, *Adv. Mater.*, 2013, **25**, 4966-
285 4985.
- 286 3 C. K. Chan, H. Peng, G. Liu, K. McIlwrath, X. F. Zhang, R. A. Huggins and Y.
287 Cui, *Nat. Nanotechnol.*, 2008, **3**, 31-35.
- 288 4 X. H. Liu, H. Zheng, L. Zhong, S. Huang, K. Karki, L. Q. Zhang, Y. Liu, A.
289 Kushima, W. T. Liang, J. W. Wang, J.-H. Cho, E. Epstein, S. A. Dayeh, S. T.
290 Picraux, T. Zhu, J. Li, J. P. Sullivan, J. Cumings, C. Wang, S. X. Mao, Z. Z. Ye, S.
291 Zhang and J. Y. Huang, *Nano Lett.*, 2011, **11**, 3312-3318.
- 292 5 X. H. Liu, L. Zhong, S. Huang, S. X. Mao, T. Zhu and J. Y. Huang, *ACS Nano*,
293 2012, **6**, 1522-1531.
- 294 6 M. T. McDowell, S. W. Lee, J. T. Harris, B. A. Korgel, C. Wang, W. D. Nix and
295 Y. Cui, *Nano Lett.*, 2013, **13**, 758-764.
- 296 7 H. Wu, G. Chan, J. W. Choi, I. Ryu, Y. Yao, M. T. McDowell, S. W. Lee, A.
297 Jackson, Y. Yang, L. Hu and Y. Cui, *Nat. Nanotechnol.*, 2012, **7**, 310-315.
- 298 8 S.-H. Ng, J. Wang, D. Wexler, K. Konstantinov, Z.-P. Guo and H.-K. Liu, *Angew.*
299 *Chem. Int. Ed.*, 2006, **45**, 6896-6899.
- 300 9 M. Gu, Y. Li, X. Li, S. Hu, X. Zhang, W. Xu, S. Thevuthasan, D. R. Baer, J.-G.
301 Zhang, J. Liu and C. Wang, *ACS Nano*, 2012, **6**, 8439-8447.
- 302 10 N. Liu, H. Wu, M. T. McDowell, Y. Yao, C. Wang and Y. Cui, *Nano Lett.*, 2012,
303 **12**, 3315-3321.
- 304 11 M. E. Stournara, Y. Qi and V. B. Shenoy, *Nano Lett.*, 2014, **14**, 2140-2149.
- 305 12 I. H. Son, J. H. Park, S. Kwon, S. Park, M. H. Rummeli, A. Bachmatiuk, H. J.
306 Song, J. Ku, J. W. Choi, J.-m. Choi, S.-G. Doo and H. Chang, *Nat. Commun.*,
307 2015, **6**.

- 308 13 C.-M. Wang, X. Li, Z. Wang, W. Xu, J. Liu, F. Gao, L. Kovarik, J.-G. Zhang, J.
309 Howe, D. J. Burton, Z. Liu, X. Xiao, S. Thevuthasan and D. R. Baer, *Nano Lett.*,
310 2012, **12**, 1624-1632.
- 311 14 L. Luo, H. Yang, P. Yan, J. J. Travis, Y. Lee, N. Liu, D. M. Piper, S.-H. Lee, P.
312 Zhao, S. M. George, J.-G. Zhang, Y. Cui, S. Zhang, C. Ban and C.-M. Wang, *ACS*
313 *Nano*, 2015, **9**, 5559-5566.
- 314 15 X. H. Liu, Y. Liu, A. Kushima, S. Zhang, T. Zhu, J. Li and J. Y. Huang, *Adv.*
315 *Energy Mater.*, 2012, **2**, 722-741.
- 316 16 Q. Li, P. Wang, Q. Feng, M. Mao, J. Liu, S. X. Mao and H. Wang, *Chem. Mater.*,
317 2014, **26**, 4102-4108.
- 318 17 H. Yang, S. Huang, X. Huang, F. Fan, W. Liang, X. H. Liu, L.-Q. Chen, J. Y.
319 Huang, J. Li, T. Zhu and S. Zhang, *Nano Lett.*, 2012, **12**, 1953-1958.
- 320 18 H. Yang, F. Fan, W. Liang, X. Guo, T. Zhu and S. Zhang, *J. Mech. Phys. Solids*,
321 2014, **70**, 349-361.
- 322 19 Q. Li, W. Li, Q. Feng, P. Wang, M. Mao, J. Liu, L. Zhou, H. Wang and H. Yao,
323 *Carbon*, 2014, **80**, 793-798.
- 324 20 X.-Y. Zhou, J.-J. Tang, J. Yang, J. Xie and L.-L. Ma, *Electrochim. Acta*, 2013, **87**,
325 663-668.
- 326 21 M. N. Obrovac and L. Christensen, *Electrochem. Solid-State Lett.*, 2004, **7**, A93-
327 A96.
- 328 22 M. T. McDowell, I. Ryu, S. W. Lee, C. Wang, W. D. Nix and Y. Cui, *Adv. Mater.*,
329 2012, **24**, 6034-6041.
- 330 23 X. H. Liu, J. W. Wang, S. Huang, F. Fan, X. Huang, Y. Liu, S. Krylyuk, J. Yoo, S.
331 A. Dayeh, A. V. Davydov, S. X. Mao, S. T. Picraux, S. Zhang, J. Li, T. Zhu and J.
332 Y. Huang, *Nat. Nanotechnol.*, 2012, **7**, 749-756.
- 333 24 K. Karki, E. Epstein, J.-H. Cho, Z. Jia, T. Li, S. T. Picraux, C. Wang and J.
334 Cumings, *Nano Lett.*, 2012, **12**, 1392-1397.
- 335 25 J. W. Wang, Y. He, F. Fan, X. H. Liu, S. Xia, Y. Liu, C. T. Harris, H. Li, J. Y.
336 Huang, S. X. Mao and T. Zhu, *Nano Lett.*, 2013, **13**, 709-715.
- 337 26 M. G. Fyta, I. N. Remediakis, P. C. Kelires and D. A. Papaconstantopoulos, *Phys.*
338 *Rev. Lett.*, 2006, **96**, 185503.
- 339 27 W. A. Brantley, *J. Appl. Phys.*, 1973, **44**, 534-535.
- 340 28 K. E. Petersen, *Proc. IEEE*, 1982, **70**, 420-457.
- 341 29 A. Kushima, J. Y. Huang and J. Li, *ACS Nano*, 2012, **6**, 9425-9432.
- 342 30 V. B. Shenoy, P. Johari and Y. Qi, *J. Power Sources*, 2010, **195**, 6825-6830.
- 343 31 M. J. Chon, V. A. Sethuraman, A. McCormick, V. Srinivasan and P. R. Guduru,
344 *Phys. Rev. Lett.*, 2011, **107**, 045503.
- 345 32 S. K. Soni, B. W. Sheldon, X. Xiao, M. W. Verbrugge, D. Ahn, H. Haftbaradaran
346 and H. Gao, *J. Electrochem. Soc.*, 2012, **159**, A38-A43.
- 347 33 M. A. Meyers and K. K. Chawla, *Mechanical Behavior of Materials*, Cambridge
348 University Press, New York, 2009.
- 349 34 S. Cho, I. Chasiotis, T. A. Friedmann and J. P. Sullivan, *J. Micromech. Microeng.*,
350 2005, **15**, 728-735.
- 351 35 T. L. Anderson, *Fracture Mechanics: Fundamentals and Applications*, CRC Press,
352 Boca Raton, 2005.

- 353 36 K. Zhao, M. Pharr, Q. Wan, W. L. Wang, E. Kaxiras, J. J. Vlassak and Z. Suo, *J.*
354 *Electrochem. Soc.*, 2012, **159**, A238-A243.
355 37 M. Pharr, Z. Suo and J. J. Vlassak, *Nano Lett.*, 2013, **13**, 5570-5577.
356 38 N. K. Simha, F. D. Fischer, O. Kolednik and C. R. Chen, *J. Mech. Phys. Solids*,
357 2003, **51**, 209-240.